

New High Nuclearity Platinum–Ruthenium Carbonyl Cluster Complexes Containing a Phenylacetylene Ligand: Structures and Properties

Richard D. Adams,* Burjor Captain, and Lei Zhu

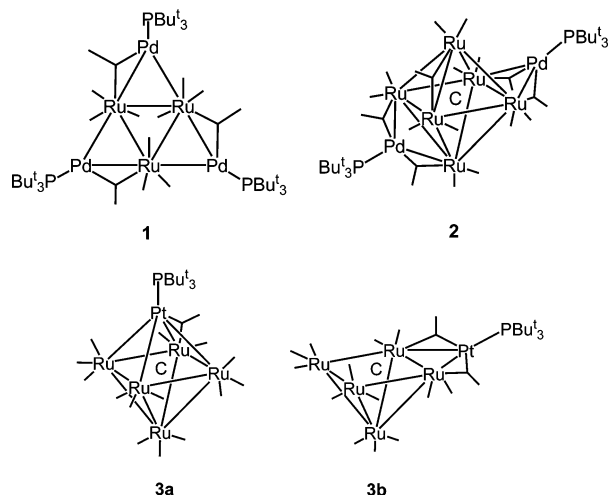
Department of Chemistry and Biochemistry, University of South Carolina,
Columbia, South Carolina 29208

Received March 9, 2005

Reaction of the mixed-metal carbonyl cluster complex $\text{Ru}_5(\text{CO})_{15}(\text{C})[\text{Pt}(\text{PBu}^t_3)]$, **3**, with PhC_2H yielded the new compound $\text{PtRu}_5(\text{CO})_{13}(\text{PBu}^t_3)(\mu_5\text{-C})(\mu_3\text{-PhC}_2\text{H})$, **4**, in 41% yield. Two new bimetallic cluster complexes, $\text{Pt}_2\text{Ru}_5(\text{CO})_{13}(\text{PBu}^t_3)_2(\mu_5\text{-C})(\mu_3\text{-PhC}_2\text{H})$, **5**, and $\text{Pt}_3\text{Ru}_5(\text{CO})_{13}(\text{PBu}^t_3)_3(\mu_5\text{-C})(\mu_3\text{-PhC}_2\text{H})$, **6**, were subsequently obtained in 44% and 40% yield, respectively, from the reaction of **4** with an excess of $\text{Pt}(\text{PBu}^t_3)_2$. All products were characterized crystallographically by single-crystal X-ray diffraction techniques. The structure of **4** consists of a square-pyramidal cluster of five ruthenium atoms with a $\text{Pt}(\text{PBu}^t_3)$ group capping one of the Ru_3 triangles. A PhC_2H ligand bridges one of the PtRu_2 triangles. Compounds **5** and **6** are similar to **4** but have in addition one and two $\text{Pt}(\text{PBu}^t_3)$ groups bridging one and two edges of the Ru_5 square-pyramidal portion of the cluster. Compound **6** was shown to be dynamically active on the ^{31}P NMR time scale by a process that involves an interchange of two of its inequivalent $\text{Pt}(\text{PBu}^t_3)$ groups.

Introduction

In recent studies we have shown that the compounds $\text{M}(\text{PBu}^t_3)_2$, $\text{M} = \text{Pt}$ or Pd , readily form higher nuclearity bimetallic cluster complexes by adding electronically unsaturated $\text{M}(\text{PBu}^t_3)$ groups across existing metal–metal bonds.^{1–3} Examples of some of these compounds include $\text{Ru}_3(\text{CO})_{12}[\text{Pd}(\text{PBu}^t_3)]_3$, **1**,¹ $\text{Ru}_6(\text{CO})_{17}(\mu_6\text{-C})[\text{Pd}(\text{PBu}^t_3)]_2$, **2**,¹ and $\text{Ru}_5(\text{CO})_{15}(\text{C})[\text{Pt}(\text{PBu}^t_3)]$, **3**.² Interestingly, compound **3** exists in solution as a mixture of two isomers, closed **3a** and open **3b**, that interconvert rapidly on the NMR time scale.²



Alkynes are very effective bridging ligands in metal carbonyl cluster complexes,^{4,5} and thus their complexes

are often the subject of studies to produce catalytic alkyne hydrogenation.⁶ The reaction of **3** with PhC_2H has been shown to yield the alkyne complex $\text{PtRu}_5(\text{CO})_{13}(\text{PBu}^t_3)(\mu_5\text{-C})(\mu_3\text{-PhC}_2\text{H})$, **4**, which is a catalyst precursor for the hydrogenation of PhC_2H to styrene and ethylbenzene.⁷ Here we report the details of the synthesis and structure of **4** as well as the synthesis and structures of two new bimetallic complexes, $\text{Pt}_2\text{Ru}_5(\text{CO})_{13}(\text{PBu}^t_3)_2(\mu_5\text{-C})(\mu_3\text{-PhC}_2\text{H})$, **5**, and $\text{Pt}_3\text{Ru}_5(\text{CO})_{13}(\text{PBu}^t_3)_3(\mu_5\text{-C})(\mu_3\text{-PhC}_2\text{H})$, **6**, obtained from reactions of **4** with $\text{Pt}(\text{PBu}^t_3)_2$.

Experimental Section

General Data. All the reactions were performed under a nitrogen atmosphere using Schlenk techniques. Reagent grade solvents were dried by standard procedures and were freshly distilled prior to use. Infrared spectra were recorded on an Avatar 360 FT-IR spectrophotometer. ^1H NMR and $^{31}\text{P}\{^1\text{H}\}$ NMR were recorded on a Varian Mercury 400 spectrometer operating at 400 and 162 MHz, respectively. $^{31}\text{P}\{^1\text{H}\}$ NMR spectra were externally referenced against 85% *ortho*- H_3PO_4 . $^{31}\text{P}\{^1\text{H}\}$ NMR spectra at various temperatures were recorded

(2) Adams, R. D.; Captain, B.; Fu, W.; Pellechia, P. J.; Smith, M. D. *Inorg. Chem.* **2003**, *42*, 2094.

(3) Adams, R. D.; Captain, B.; Fu, W.; Smith, M. D. *J. Organomet. Chem.* **2003**, *682*, 113.

(4) (a) Deabate, S.; Giordano, R.; Sappa, E. *J. Cluster Sci.* **1997**, *8*, 407. (b) Sappa, E. *J. Cluster Sci.* **1994**, *5*, 211.

(5) (a) Mallors, R. L.; Blake, A. J.; Parsons, S.; Johnson, B. F. G.; Dyson, P. J.; Braga, D.; Grepioni, F.; Parisini, E. *J. Organomet. Chem.* **1997**, *532*, 133. (b) Drake, S. R.; Johnson, B. F. G.; Lewis, J.; Conole, G.; McPartlin, M. *J. Chem. Soc., Dalton Trans.* **1990**, 995. (c) Vargas, M. D.; Nicholls, J. N. *Adv. Inorg. Chem.* **1986**, *30*, 123.

(6) (a) Adams, R. D.; Barnard, T. S.; Li, Z.; Wu, W.; Yamamoto, J. *J. Am. Chem. Soc.* **1994**, *116*, 9103. (b) Blazina, D.; Duckett, S. B.; Dyson, P. J.; Lohman, J. A. B. *J. Chem. Soc., Dalton Trans.* **2004**, 2108. (c) Blazina, D.; Duckett, S. B.; Dyson, P. J.; Lohman, J. A. B. *Chem. Eur. J.* **2003**, *9*, 1046. (d) Ferrand, V.; Süß-Fink, G.; Neels, A.; Stoeckli-Evans, H. *J. Chem. Soc., Dalton Trans.* **1998**, 3825.

(7) Adams, R. D.; Captain, B.; Zhu, L. *J. Am. Chem. Soc.* **2004**, *126*, 3042.

* To whom correspondence should be addressed. E-mail: Adams@mail.chem.sc.edu.

(1) (a) Adams, R. D.; Captain, B.; Fu, W.; Hall, M. B.; Manson, J.; Smith, M. D.; Webster, C. E. *J. Am. Chem. Soc.* **2004**, *126*, 5253.

Table 1. Crystallographic Data for Compounds 4, 5, and 6

	4	5	6
empirical formula	PtRu ₅ PO ₁₃ C ₃₄ H ₃₃ ^{1/2} C ₈ H ₁₈	Pt ₂ Ru ₅ P ₂ O ₁₃ C ₄₆ H ₆₀ ·C ₆ H ₁₄	Pt ₃ Ru ₅ P ₃ O ₁₃ C ₅₈ H ₈₇ ^{1/2} C ₆ H ₆
fw	1438.13	1864.58	2214.86
cryst syst	triclinic	monoclinic	triclinic
lattice params			
<i>a</i> (Å)	12.6218(5)	39.0570(13)	14.7755(8)
<i>b</i> (Å)	13.3776(5)	18.0757(6)	16.3794(9)
<i>c</i> (Å)	14.3656(5)	22.9961(7)	17.372(1)
α (deg)	92.678(1)	90	80.340(1)
β (deg)	91.051(1)	126.005(1)	66.324(1)
γ (deg)	109.958(1)	90	71.645(1)
<i>V</i> (Å ³)	2275.91(15)	13133.4(7)	3650.4(4)
space group	<i>P</i> $\bar{1}$	<i>C</i> 2/ <i>c</i>	<i>P</i> 1
<i>Z</i> value	2	8	2
ρ _{calc} (g/cm ³)	2.099	1.886	2.015
μ(Mo Kα) (mm ⁻¹)	4.771	5.463	6.849
temperature (K)	296	296	296
2θ _{max} (deg)	56.6	50.06	56.6
no. obs (<i>I</i> > 2σ(<i>I</i>))	9150	6077	13974
no. params	515	655	778
goodness of fit, GOF ^a	1.037	1.095	1.019
max. shift in cycle	0.001	0.007	0.005
residuals: ^a R1; wR2	0.0454; 0.1139	0.0509; 0.1155	0.0485; 0.1275
absorp corr, max./min.	SADABS 1.000/0.794	SADABS 1.000/0.340	SADABS 1.000/0.553
largest peak in final diff map (e ⁻ /Å ³)	5.424	1.973	7.503

^a $R = \sum_{hkl} (|F_{\text{obs}}| - |F_{\text{calc}}|) / \sum_{hkl} |F_{\text{obs}}|$; $R_w = [\sum_{hkl} w(|F_{\text{obs}}| - |F_{\text{calc}}|)^2 / \sum_{hkl} w F_{\text{obs}}^2]^{1/2}$, $w = 1/\sigma^2(F_{\text{obs}})$. GOF = $[\sum_{hkl} w(|F_{\text{obs}}| - |F_{\text{calc}}|)^2 / (n_{\text{data}} - n_{\text{vari}})]^{1/2}$.

on a Varian Innova 500 spectrometer operating at 202.5 MHz. Elemental analyses were performed by Desert Analytics (Tucson, AZ). The mass spectral measurements performed by direct exposure probe using electron impact ionization (EI) were made on a VG 70S instrument. Pt(PBu₃)₂ and phenylacetylene were purchased from Strem and Aldrich, respectively, and were used without further purification. Ru₅(CO)₁₅(C)[Pt(PBu₃)₃], **3**, was prepared according to a previously reported procedure.² Product separations were performed by TLC in air on Analtech 0.25 and 0.5 mm silica gel 60 Å F₂₅₄ glass plates.

Synthesis of PtRu₅(CO)₁₃(PBu₃)₃(μ₅-C)(μ₃-PhC₂H), 4. A 16 mg amount of **3** (0.012 mmol) was dissolved in 20 mL of CH₂Cl₂ in a 50 mL three-neck flask. Phenylacetylene (0.010 mL, 0.090 mmol) was added to the solution, which was then heated to reflux for 1 h. After cooling, the solvent was removed in vacuo, and the product was separated by TLC by using 6:1 hexane–methylene chloride solvent mixture to yield 6.8 mg (41%) of PtRu₅(CO)₁₃(PBu₃)₃(μ₅-C)(μ₃-PhC₂H), **4**. Spectral data for **4**: IR ν_{CO} (cm⁻¹ in CH₂Cl₂): 2076 (vs), 2044 (vs), 2027 (s), 2014 (vs), 1985 (w, sh), 1955 (vw, sh). ¹H NMR (in CDCl₃): δ 8.58 (d, 1H, CH, ³J_{P-H} = 16 Hz), 7.3–7.4 (m, 5H, Ph), 1.50 (d, 27H, CH₃, ³J_{P-H} = 13 Hz). ³¹P{¹H} NMR (in CDCl₃): δ 113.4 (s, 1P, ¹J_{Pt-P} = 4545 Hz). Anal. Calcd: C, 29.57; H, 2.39. Found: C, 28.47; H, 2.15. EI-MS showed the parent ion at *m/z* 1381 and ions corresponding to loss of 13 CO ligands. The observed isotope pattern is consistent with that expected for the presence of one platinum and five ruthenium atoms.

Synthesis of Pt₂Ru₅(CO)₁₃(PBu₃)₂(μ₅-C)(μ₃-PhC₂H), 5, and Pt₃Ru₅(CO)₁₃(PBu₃)₃(μ₅-C)(μ₃-PhC₂H), 6. A 12.0 mg amount of **4** (0.0086 mmol) was dissolved in 20 mL of CH₂Cl₂ in a 50 mL three-neck flask. A 5.2 mg amount of Pt(PBu₃)₂ (0.086 mmol) was added, and the solution was heated to reflux for 30 min. The solvent was removed in vacuo, and the products were isolated by TLC by using 6:1 hexane–methylene chloride solvent mixture to yield in order of elution 8.8 mg (57%) of a red **5** and 1.6 mg (8%) of a red **6**. Spectral data for **5**: IR ν_{CO} (cm⁻¹ in CH₂Cl₂): 2060 (m), 2049 (w), 2021 (vs), 2002 (s), 1973 (w, sh), 1845 (w), 1814 (w). ¹H NMR (in toluene-*d*₈): δ 8.70 (d, 1H, CH, ³J_{P-H} = 16 Hz), 7.00–7.61 (m, Ph), 1.40 (d, 27H, CH₃, ³J_{P-H} = 13 Hz), 1.16 (d, 27H, CH₃, ³J_{P-H} = 13 Hz). ³¹P{¹H} NMR (in toluene-*d*₈): δ 113.8 (s, 1P, ¹J_{Pt-P} = 5783 Hz), 111.5 (s, 1P, ¹J_{Pt-P} = 4551 Hz). Anal. Calcd for **5**: C, 31.06; H, 3.38. Found: C, 30.81; H, 3.24. Spectral data for **6**: IR ν_{CO} (cm⁻¹ in CH₂Cl₂): 2026 (s), 2003 (s, sh), 1990 (vs), 1844 (w,

br), 1825 (w, br), 1801 (w, br). ¹H NMR (in toluene-*d*₈): δ 9.1 (d, 1H, CH, ³J_{P-H} = 16 Hz), 7.25–7.99 (m, Ph), 1.47 (d, 27H, CH₃, ³J_{P-H} = 13 Hz), 1.18 (d, 27H, CH₃, ³J_{P-H} = 13 Hz). ³¹P{¹H} NMR (in toluene-*d*₈ at -35 °C): δ 112.1 (s, 1P, ¹J_{Pt-P} = 5650 Hz), 109.7 (s, 1P, ¹J_{Pt-P} = 5809 Hz), 108.0 (s, 1P, ¹J_{Pt-P} = 4532 Hz). Anal. Calcd for **6**: C, 32.01; H, 4.00. Found: C, 32.40; H, 4.05.

Synthesis of 6 in a Higher Yield. A 19.5 mg amount of **4** (0.014 mmol) was dissolved in 25 mL of CH₂Cl₂ in a 50 mL three-neck flask. An excess of Pt(PBu₃)₂ (33.0 mg, 0.055 mmol) was then added, and the reaction solution was allowed to stir for 12 h at room temperature. The solvent was then removed in vacuo, and the products were separated by TLC by using 5:1 hexane–methylene chloride solvent mixture to yield 12.1 mg (40%) of red **6** and 11.1 mg (44%) of red **5**.

Conversion of 5 into 6. A 12.8 mg amount of **5** (0.0072 mmol) was dissolved in 10 mL of CH₂Cl₂ in a 25 mL three-neck flask. An excess of Pt(PBu₃)₂ (8.6 mg, 0.144 mmol) was added to the solution. The reaction continued for 5 h at room temperature. The solvent was then removed in vacuo, and the products were separated by TLC by using 5:1 hexane–methylene chloride solvent mixture to yield 7.4 mg (47%) of red **6**.

Crystallographic Analyses. Dark red crystals of **4** suitable for diffraction analysis were grown by slow evaporation of solvent from a benzene–octane solution at 8 °C. Dark red single crystals of **5** suitable for diffraction analysis were grown by slow evaporation of solvent from a methylene chloride–hexane solution at -20 °C. Dark red crystals of **6** suitable for diffraction analysis were grown by slow evaporation of solvent from a benzene–octane solution at 8 °C. Each data crystal was glued onto the end of a thin glass fiber. X-ray intensity data were measured using a Bruker SMART APEX CCD-based diffractometer using Mo Kα radiation (λ = 0.71073 Å). The raw data frames were integrated with the SAINT+ program by using a narrow-frame integration algorithm.⁸ Corrections for Lorentz and polarization effects were also applied by SAINT. An empirical absorption correction based on the multiple measurement of equivalent reflections was applied by using the program SADABS. All structures were solved by a combination of direct methods and difference Fourier syntheses and refined by full-matrix least-squares on *F*², by

(8) SAINT+, version 6.2a; Bruker Analytical X-ray Systems, Inc., Madison, WI, 2001.

using the SHELXTL software package.⁹ Crystal data, data collection parameters, and results of the analyses for compounds are listed in Table 1.

Compounds **4** and **6** crystallized in the triclinic crystal system. The space group $P\bar{1}$ was assumed and confirmed by the successful solution and refinement of the structure in both cases. All non-hydrogen atoms were refined with anisotropic displacement parameters. The hydrogen atom on the phenylacetylene ligand was located and refined with an isotropic displacement parameter in both compounds. Hydrogen atoms were placed in geometrically idealized positions and refined as standard riding atoms. Compound **4** cocrystallized with half a molecule of octane from the crystallization solvent in the asymmetric crystal unit. The octane molecule was refined with isotropic displacement parameters. Five geometric restraints were used in modeling the octane molecule, which was disordered about an inversion center. Compound **6** cocrystallized with half a molecule of benzene from the crystallization solvent in the asymmetric crystal unit. The benzene molecule was refined with isotropic displacement parameters. There is only one large peak in the final difference map, $7.503 \text{ e}^-/\text{\AA}^3$ located 0.82 \AA from Pt1, which is structurally unimportant. This may be a consequence of a site-occupancy disorder near Pt1 which was not modeled.

Compound **5** crystallized in the monoclinic crystal system. The systematic absences were consistent with either of the space groups $C2/c$ or Cc . $C2/c$ was selected initially, and the structure was solved and successfully refined in this space group. All non-hydrogen atoms were refined with anisotropic thermal parameters. Compound **5** cocrystallized with a molecule of hexane from the crystallization solvent in the asymmetric crystal unit. This hexane unit was included in the analysis and was refined with isotropic thermal parameters. Nine geometric restraints were used in modeling the hexane solvent molecule. Hydrogen atoms were placed in geometrically idealized positions and included as standard riding atoms.

Results and Discussion

The PhC_2H complex $\text{PtRu}_5(\text{CO})_{13}(\text{PBUt}_3)_3(\mu_5\text{-C})(\mu_3\text{-PhC}_2\text{H})$, **4**, was obtained in 41% yield from the reaction of **3** with PhC_2H in a CH_2Cl_2 solution at reflux. Compound **4** was characterized by a combination of IR, ^1H NMR, ^{31}P NMR, and single-crystal X-ray diffraction analyses. An ORTEP diagram of the molecular structure of **4** is shown in Figure 1. The molecule consists of a square-pyramidal cluster of five ruthenium atoms with an interstitial carbido ligand C(1) in the center. There is a platinum Pt(1) capping the Ru_3 triangle Ru(1), Ru(2), Ru(3). A PBUt_3 ligand is coordinated to the platinum atom, and a PhC_2H ligand bridges one of the PtRu_2 triangles, Pt(1)–C(3) = $1.980(7) \text{ \AA}$, Ru(2)–C(3) = $2.210(7) \text{ \AA}$, Ru(2)–C(2) = $2.214(6) \text{ \AA}$, C(2)–C(3) = $1.369(10) \text{ \AA}$. The hydrogen atom H(1) was located and refined. As expected, H(1) exhibits a very low-field resonance in the ^1H NMR spectrum of **4**, $\delta = 8.58$, with coupling to the phosphorus atom of the neighboring PBUt_3 ligand, $^3J_{\text{P-H}} = 16 \text{ Hz}$. A single resonance was found in the $^{31}\text{P}\{^1\text{H}\}$ NMR spectrum, $\delta = 113.4$, that showed strong coupling to ^{195}Pt , $^1J_{\text{Pt-P}} = 4545 \text{ Hz}$. Overall, compound **4** contains a total of 86 valence electrons, which is precisely the number expected for a metal-capped square-pyramidal cluster of five metal atoms.¹⁰ The structure of **4** seems to suggest that this compound was formed by the addition of a PhC_2H

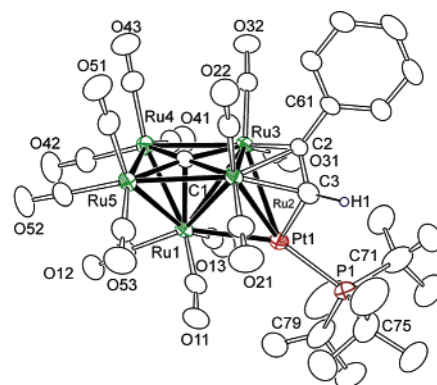
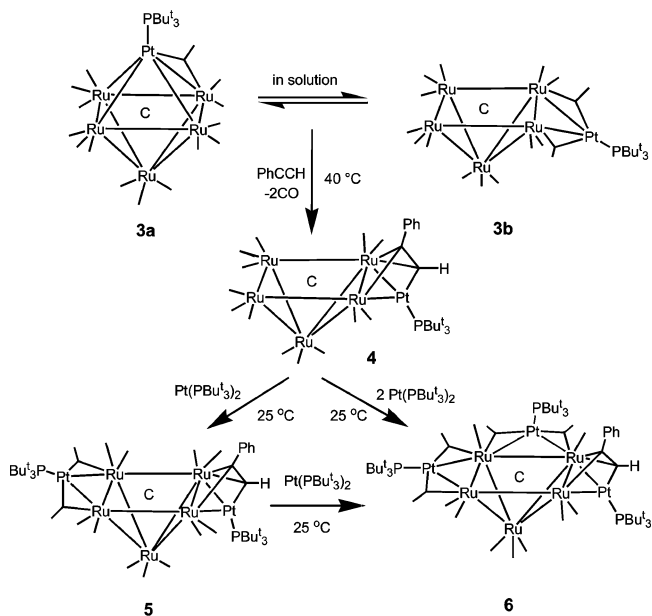


Figure 1. ORTEP diagram of **4** showing 30% probability thermal ellipsoids. Selected interatomic distances (\AA): Pt(1)–C(3) = $1.980(7)$, Pt(1)–P(1) = $2.3122(19)$, Pt(1)–Ru(1) = $2.6787(6)$, Pt(1)–Ru(2) = $2.8476(6)$, Pt(1)–Ru(3) = $2.9979(5)$, Ru(1)–Ru(5) = $2.7705(8)$, Ru(1)–Ru(4) = $2.7949(8)$, Ru(1)–Ru(2) = $2.9856(7)$, Ru(1)–Ru(3) = $3.0018(7)$, Ru(2)–Ru(3) = $2.6666(7)$, Ru(2)–Ru(5) = $2.8926(7)$, Ru(3)–Ru(4) = $2.9037(7)$, Ru(4)–Ru(5) = $2.8898(8)$, Ru(2)–C(3) = $2.210(7)$, Ru(2)–C(2) = $2.214(6)$, C(2)–C(3) = $1.369(10)$.

Scheme 1



molecule to the electron-deficient platinum atom of the “open” isomer of **3**, **3b** (see Scheme 1), but one cannot rule out that the PhC_2H molecule might have actually added to the closed isomer **3a** and then converted to **4** by an intramolecular rearrangement.

Two new bimetallic cluster complexes, $\text{Pt}_2\text{Ru}_5(\text{CO})_{13}(\text{PBUt}_3)_2(\mu_5\text{-C})(\mu_3\text{-PhC}_2\text{H})$, **5**, and $\text{Pt}_3\text{Ru}_5(\text{CO})_{13}(\text{PBUt}_3)_3(\mu_5\text{-C})(\mu_3\text{-PhC}_2\text{H})$, **6**, were obtained in 57% and 8% yield, respectively, when a solution of **4** containing 1 equiv of $\text{Pt}(\text{PBUt}_3)_2$ in CH_2Cl_2 solvent was heated to reflux for 30 min. As expected, the yield of the triplatinum product **6** was increased (to 40%) at the expense of **5** (44%) when the amount of $\text{Pt}(\text{PBUt}_3)_2$ was significantly increased relative to that of **4**. Compounds **5** and **6** were both characterized by a combination of IR, ^1H NMR, ^{31}P NMR, and single-crystal X-ray diffraction analyses. An ORTEP diagram of the molecular structure of **5** is shown in Figure 2. Overall, this molecule is very similar to **4** except that it contains an additional $\text{Pt}(\text{PBUt}_3)$

(9) Sheldrick, G. M. *SHELXTL*, version 6.1; Bruker Analytical X-ray Systems, Inc.: Madison, WI, 1997.

(10) Mingos, D. M. P. *Acc. Chem. Res.* **1984**, *17*, 311.

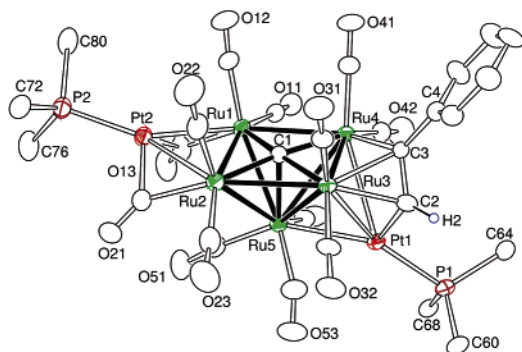


Figure 2. ORTEP diagram of **5** showing 30% probability thermal ellipsoids. The methyl groups on the PBu_3 ligand are not shown for clarity. Selected interatomic distances (Å): Pt(1)–P(1) = 2.317(3), Pt(1)–Ru(3) = 2.8698(8), Pt(1)–Ru(4) = 3.0028(8), Pt(1)–Ru(5) = 2.6699(9), Pt(1)–C(2) = 1.976(6), Pt(2)–P(2) = 2.315(3), Pt(2)–Ru(1) = 2.7465(9), Pt(2)–Ru(2) = 2.8055(9), Ru(1)–Ru(5) = 2.8181(11), Ru(1)–Ru(2) = 2.9270(11), Ru(1)–Ru(4) = 2.8909(11), Ru(2)–Ru(3) = 2.8824(12), Ru(2)–Ru(5) = 2.8094(11), Ru(3)–Ru(4) = 2.6748(10), Ru(3)–Ru(5) = 2.9484(11), Ru(4)–Ru(5) = 3.0142(10), C(2)–C(3) = 1.391(12).

group that bridges the Ru(1)–Ru(2) edge of the Ru₅ square pyramid on the side opposite the bridging PhC_2H ligand. One carbonyl ligand on Ru(1), C(13)–O(13), and one on Ru(2), C(21)–O(21), that were originally terminally coordinated in **4**, have become bridging ligands across the Pt(2)–Ru(1) and Pt(2)–Ru(2) bonds in **5**. Atom Pt(2) has formally only a 16-electron configuration and has been observed a number of times previously for the Pt containing the bulky PBu_3 ligand.^{1–3} As a result, the total valence electron count for **5** is only 98, which is two less than that expected if all of the metal atoms obeyed the skeletal electron pair theory.¹⁰ The $^{31}\text{P}\{^1\text{H}\}$ NMR spectrum of **5** exhibits two resonances at $\delta = 113.8$ (s, 1P, $^1J_{\text{Pt-P}} = 5783$ Hz), 111.5 (s, 1P, $^1J_{\text{Pt-P}} = 4551$ Hz). Because of the strong similarity of the coupling to ^{195}Pt observed for compound **4**, the latter resonance is assigned to the phosphine ligand coordinated to the platinum atom Pt(1) that contains the bridging alkyne ligand. The former is thus due to the phosphorus atom of the phosphine on the unsaturated platinum atom Pt(2). As in **4**, the hydrogen atom on the PhC_2H ligand exhibits a very low-field resonance, $\delta = 8.70$, $^3J_{\text{P-H}} = 16$ Hz, in the ^1H NMR spectrum. The $^{31}\text{P}\{^1\text{H}\}$ NMR spectrum of **5** exhibits two resonances at $\delta = 113.8$ (s, 1P, $^1J_{\text{Pt-P}} = 5783$ Hz), 111.5 (s, 1P, $^1J_{\text{Pt-P}} = 4551$ Hz).

An ORTEP diagram of the molecular structure of **6** is shown in Figure 3. Overall, this molecule is very similar to **5**, except that it contains still another $\text{Pt}(\text{PBu}_3)$ group. This one bridges the Ru(1)–Ru(4) edge of the Ru₅ square pyramid on the side adjacent to the bridging PhC_2H ligand. Thus, in **6** there are two 16-electron bridging $\text{Pt}(\text{PBu}_3)$ groups. Carbonyl ligands bridge each Pt–Ru bond to each of the unsaturated $\text{Pt}(\text{PBu}_3)$ groups, as also found in **5**. As a result, the total valence electron count for **6** is only 110, which is four less than that expected if the cluster obeyed the skeletal electron pair theory.¹⁰ The hydrogen atom on the PhC_2H ligand exhibits a very low-field resonance, $\delta = 9.1$, $^3J_{\text{P-H}} = 16$ Hz, in the ^1H NMR spectrum. The $^{31}\text{P}\{^1\text{H}\}$ NMR spectrum of **6** at -35 °C shows three resonances of equal intensity, $\delta = 112.1$, 109.7, and

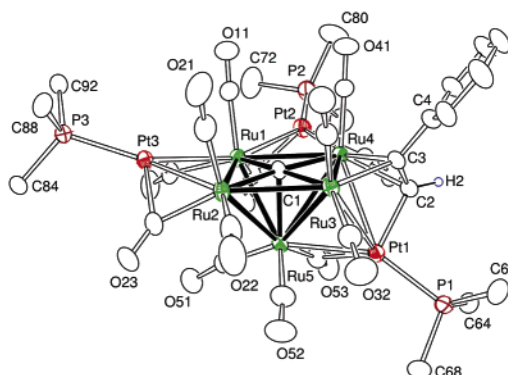


Figure 3. ORTEP diagram of **6** showing 30% probability thermal ellipsoids. The methyl groups on the PBu_3 ligand are not shown for clarity. Selected interatomic distances (Å): Pt(1)–P(1) = 2.332(2), Pt(1)–C(2) = 1.983(7), Pt(1)–Ru(3) = 2.9788(7), Pt(1)–Ru(4) = 2.9201(6), Pt(1)–Ru(5) = 2.6583(7), Pt(2)–P(2) = 2.320(2), Pt(2)–Ru(1) = 2.7780(6), Pt(2)–Ru(4) = 2.7762(6), Pt(3)–P(3) = 2.323(2), Pt(3)–Ru(1) = 2.8090(6), Pt(3)–Ru(2) = 2.7356(7), Ru(1)–Ru(2) = 2.9428(8), Ru(1)–Ru(4) = 2.9351(8), Ru(1)–Ru(5) = 2.8069(9), Ru(2)–Ru(3) = 2.8723(8), Ru(2)–C(5) = 2.8297(9), Ru(3)–Ru(4) = 2.6696(8), Ru(3)–Ru(5) = 2.9891(9), Ru(3)–C(3) = 2.087(7), Ru(4)–Ru(5) = 2.9932(8), Ru(4)–C(2) = 2.167(8), Ru(4)–C(3) = 2.215(7), C(2)–C(3) = 1.388(11).

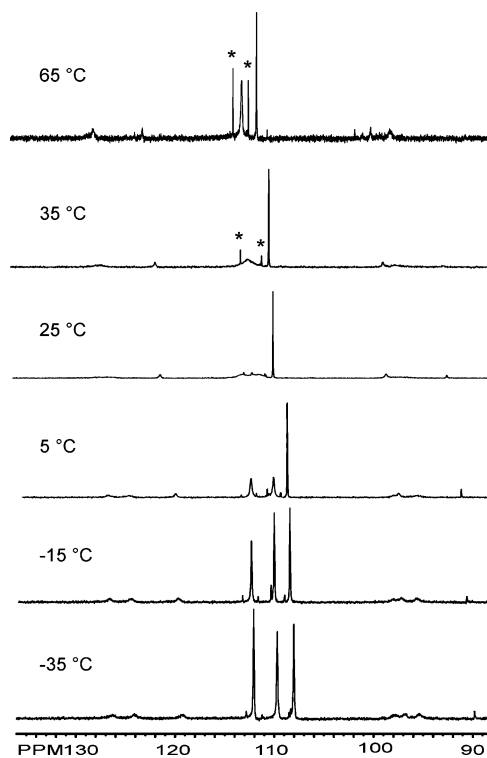
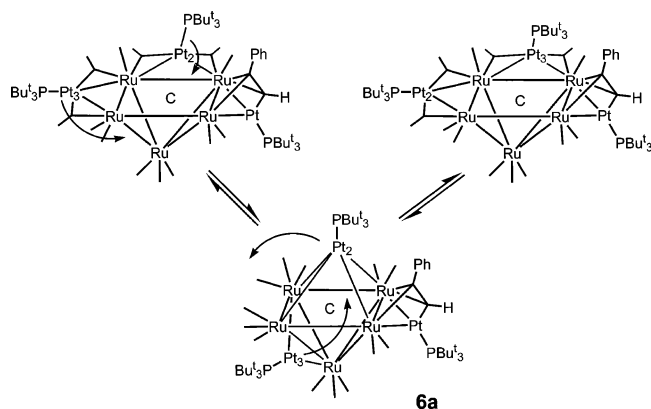


Figure 4. Variable-temperature $^{31}\text{P}\{^1\text{H}\}$ NMR spectra for compound **6**.

108.0, all showing appropriate ^{31}P – ^{195}Pt coupling indicating that each of the phosphorus atoms are bonded directly to a platinum atom. These resonances are attributed to the three inequivalent phosphine ligands. The resonance at 108.0 ppm, $^1J_{\text{Pt-P}} = 4532$ Hz, is assigned to the $\text{Pt}(\text{PBu}_3)$ group that is bonded to the phenylacetylene ligand because of the similarity of the Pt–P coupling constant to those in compounds **4** and **5**. The other two resonances are assigned to the phosphorus atoms on the unsaturated platinum atoms Pt(2) and Pt(3). It seems likely that **5** would be an intermediate

Scheme 2



in the reaction that yields **6** from **4**. This was confirmed by an independent experiment. Treatment of **5** with $\text{Pt}(\text{PBu}^t_3)_2$ yielded **6** in 47% yield.

Compound **6** exhibits a dynamical activity on the NMR time scale, as seen in the variable-temperature $^{31}\text{P}\{^1\text{H}\}$ NMR spectra shown in Figure 4. The two resonances at $\delta = 112.1$ and 109.7 broaden as the temperature is raised. They coalesce at $35\text{ }^\circ\text{C}$, and at $65\text{ }^\circ\text{C}$ they appear as a sharp singlet at $\delta = 113.1$ with $^{195}\text{Pt}-^{31}\text{P}$ coupling of 5933 Hz. However, at this temperature compound **6** undergoes decomposition to compound **5** at a significant rate, and the resonances due to **5** begin to appear in the spectrum. The rate of exchange at the coalescence temperature (k_c) was estimated by using the expression $k_c = \pi \Delta\nu_0/(2)^{1/2}$, where $\Delta\nu_0$ is the chemical shift difference between the resonances in the slow exchange limit. Substitution of k_c in the Eyring equation provides the free energy of activation for the process at the coalescence temperature, $\Delta G^\ddagger(308\text{ K}) = 13.8(5)$ kcal/mol. The dynamical spectra clearly indicate that the two unsaturated $\text{Pt}(\text{PBu}^t_3)$ groups are interchanging. This includes the platinum atoms because the $\text{Pt}-\text{P}$ coupling is still observed in the fast exchange limit.

Although there are other possibilities, one mechanism for the exchange process is shown in Scheme 2. Transformation of **6** into an isomer such as **6a** could occur simply by shifting one of the edge-bridged $\text{Pt}(\text{PBu}^t_3)$ groups on to the square base and the other across an apical–basal $\text{Ru}-\text{Ru}$ bond. The interchange is then completed by shifting these platinum groups to the sites

originally occupied by the other platinum group as indicated by the arrows in the figure. Similar processes have been proposed to explain the dynamical behavior of the $\text{Pt}(\text{PBu}^t_3)$ groups in the compounds **3**² and $(\eta^6\text{-C}_6\text{H}_6)\text{Ru}_5(\text{CO})_{12}(\text{C})[\text{Pt}(\text{PBu}^t_3)]$, **7**.¹¹

There is currently much interest in the synthesis of bimetallic cluster complexes because of their use as precursors in the preparation of hydrogenation catalysts on oxide supports.¹² It has been shown that certain bimetallic catalysts have both higher activity and better product selectivity than their monometallic counterparts.¹³ This has been attributed to synergy between the different metals.¹³ Thus, studies of the synthesis and characterization of platinum-containing bimetallic cluster complexes have received considerable attention.¹⁴

Acknowledgment. This research was supported by the Office of Basic Energy Sciences of the U.S. Department of Energy under Grant No. DE-FG02-00ER14980. We thank STREM for donation of a sample of $\text{Pt}(\text{PBu}^t_3)_2$. We wish to thank Dr. Perry J. Pellechia for his valuable assistance with the NMR studies.

Supporting Information Available: X-ray and CIF tables for the structural analyses of compounds **4**–**6**. This material is available free of charge via the Internet at <http://pubs.acs.org>.

OM050175N

(11) Adams, R. D.; Captain, B.; Pellechia, P. J.; Zhu, L. *Inorg. Chem.* **2004**, *43*, 7243.

(12) (a) Thomas, J. M.; Johnson, B. F. G.; Raja, R.; Sankar, G.; Midgley, P. A. *Acc. Chem. Res.* **2003**, *36*, 20. (b) Raja, R.; Khimyak, T.; Thomas, J. M.; Hermans, S.; Johnson, B. F. G. *Angew. Chem., Int. Ed.* **2001**, *40*, 4638. (c) Hermans, S.; Raja, R.; Thomas, J. M.; Johnson, B. F. G.; Sankar, G.; Gleeson, D. *Angew. Chem., Int. Ed.* **2001**, *40*, 1211. (d) Shephard, D. S.; Maschmeyer, T.; Johnson, B. F. G.; Thomas, J. M.; Sankar, G.; Ozkaya, D.; Zhou, W.; Oldroyd, R. D.; Bell, R. D. *Angew. Chem., Int. Ed. Engl.* **1997**, *36*, 2242. (e) Shephard, D. S.; Maschmeyer, T.; Sankar, G.; Thomas, J. M.; Ozkaya, D.; Johnson, B. F. G.; Raja, R.; Oldroyd, R. D.; Bell, R. G. *Chem. Eur. J.* **1998**, *4*, 12. (f) Braunstein, P.; Rosé, J. In *Catalysis and Related Reactions with Compounds Containing Heteronuclear Metal–Metal Bonds*, in *Comprehensive Organometallic Chemistry II*; Wilkinson, Stone, Abel, Eds.; Elsevier: New York, 1995; Vol 10, Chapter 7. (g) Braunstein, P.; Rose, J. In *Catalysis by Di- and Polynuclear Metal Cluster Complexes*; Adams, R. D., Cotton, F. A., Eds.; VCH: New York, 1998; Chapter 13, p 443.

(13) (a) Raja, R.; Sankar, G.; Hermans, S.; Shephard, D. S.; Bromley, S.; Thomas, J. M.; Johnson, B. F. G. *Chem. Commun.* **1999**, 1571. (b) Alexeev, O. S.; Gates, B. C. *Ind. Eng. Chem. Res.* **2003**, *42*, 1571. (c) Ichikawa, M. *Adv. Catal.* **1992**, *38*, 283.

(14) (a) Adams, R. D. In *Comprehensive Organometallic Chemistry II*; Abel, E. W., Stone, F. G. A., Wilkinson, G., Eds.; Pergamon: Oxford, 1995; Vol 10, p 1. (b) Farrugia, L. J. *Adv. Organomet. Chem.* **1990**, *31*, 301.